Graphical Model for Estimating Oral Bioavailability of Drugs in Humans and Other Species from Their Caco-2 Permeability and in Vitro Liver Enzyme Metabolic Stability Rates

Arun K. Mandagere,*,† Thomas N. Thompson,‡ and Kin-Kai Hwang§

Pfizer Global Research and Development, 2800 Plymouth Road, Ann Arbor, Michigan 48105, Quintiles, Box 9708, Kansas City, Missouri 64134, and Aventis Pharmaceutical, P.O. Box 6800, Bridgewater, New Jersey 08807

Received April 2, 2001

This paper describes a graphical model for simplifying in vitro absorption, metabolism, distribution, and elimination (ADME) data analysis through the estimation of oral bioavailability (%*F*) of drugs in humans and other species. This model integrates existing in vitro ADME data, such as Caco-2 permeability (P_{app}) and metabolic stability (percent remaining − %*R*) in liver S9 or microsomes, to estimate %*F* into groups of low, medium, or high regions. To test the predictive accuracy of our model, we examined 21 drugs and drug candidates with a wide range of oral bioavailability values, which represent approximately 10 different therapeutic areas in humans, rats, dogs, and guinea pigs. In vitro data from model compounds were used to define the boundaries of the low, medium, and high regions of the %*F* estimation plot. On the basis of the in vitro data, warfarin (93%), indomethacin (98%), timolol (50%), and carbamazepine (70%) were assigned to the high %*F* region; propranolol (26%) and metoprolol (38%) to medium %*F* region; and verapamil (22%) and mannitol (18%) to the low %*F* region. Similarly, the %*F* of 11 drug candidates from Elastase Inhibitor, NK1/NK2 antagonist, and anti-viral projects in rats, guinea pigs, and dogs were correctly estimated. This model estimates the oral bioavailability ranges of neutral, polar, esters, acidic, and basic drugs in all species. For a large number of drug candidates, this graphical model provides a tool to estimate human oral bioavailability from in vitro ADME data. When combined with the high throughput in vitro ADME screening process, it has the potential to significantly accelerate the processes of lead identification and optimization.

Introduction

In the pharmaceutical industry, the drug discovery and development process has undergone a major change with the advent of combinatorial chemistry and high throughput pharmacological screens (HTS). Thus, a much larger number of compounds with good potency and specificity are identified through HTS. Despite the availability of large pools of active compounds, only a limited number of these compounds are evaluated in animal models due to the severe capacity limits of in vivo studies. Lead compounds that are selected based on animal studies are not guaranteed similar results in humans. In part, this can be explained by the well-known fact that a poor correlation exists between animal and human bioavailability, probably due to large differences in metabolism among species.[1]

Generally, the key selection criterion is for compounds that exhibit the greatest potency in vitro. However, reliance solely on potency data may contribute to the high failure rate of drugs in development. In fact, recent reports suggest that the success rate in developing drugs from the lead candidate stage to market is only 10−20%.[2,3] While many factors contribute to a high failure rate, it is somewhat surprising to note that poor pharmacokinetic (PK) properties, such as poor oral bioavailability or duration of action, account for nearly half of the failures in clinical development.[2,3]

Therefore, it is essential that absorption, metabolism, distribution, and elimination (ADME) (PK) and physiochemical data be available to medicinal chemists early in the discovery stage. At this point, information can be utilized to synthesize new structural analogues to improve those properties by using principles of rational drug design. While the ideal would be to screen a large number of drug candidates by in vivo PK studies, the in vivo model is impractical because these studies are inherently slow, labor intensive, and not amenable to automation.

In response to this need, the concept of in vivo cassette dosing is being employed to increase the throughput of PK studies.[4−6] While in vivo cassette dosing results in throughput improvement, it too has limitations. Overall throughput capacity is still limited, potential drug interactions could lead to erroneous PK assessment and compound requirement increases, and there are a limited number of species available with this method. Clearly, a model for predicting human bioavailability and PK parameters would be highly advantageous for selecting lead candidates. This model must have a high probability of success for selecting candidates while rejecting those with low probabilities of success.

In order for potential new drugs to be bioavailable, they must be effectively absorbed and have good meta-

* To whom correspondence should be addressed. Phone: 734-622-1626. Fax: 734-622-3244. E-mail: arun.mandagere@Pfizer.com.
† Pfizer Global Research and Development.
‡ Quintiles.
§ Aventis Pharmaceutical.

10.1021/jm010152k CCC: $22.00
Published on Web 12/20/2001

bolic stability. Fortunately, there are many screening techniques based on these properties which can be used to improve the ability to recognize which compounds may be bioavailable. For example, to identify absorption issues, there are three approaches: (1) computational models, (2) direct models—such as screens for poor solubility with high throughput turbidimetric solubility,[7] and (3) in vitro evaluations of permeability that use Caco-2 cells or in situ gut loop.[8,9] To characterize metabolism parameters such as metabolic clearance and first-pass metabolism, scientists use metabolic screens based on liver enzyme preparations (S9 and microsomes) or hepatocytes.[10,11] In vitro absorption and metabolism studies can be automated and thus have sufficient throughput capacity to screen a much larger number of compounds than by in vivo studies.[12−15] In vitro screens provide specific information, i.e., rates of permeability and metabolism, in a very timely manner, although there are limitations in the depth of this information and more extensive studies are generally warranted once compounds have been identified for further development.

Investigations have demonstrated excellent correlation between Caco-2 permeability and extent of absorption in humans.[16] Other correlations include permeability in human and rabbit colon,[17] and the fraction of oral dose absorbed between humans and rats[18] for passively diffused compounds. Similarly, recent metabolism studies with human hepatocytes demonstrate that in vitro intrinsic clearance correlates with broad ranges of low, intermediate, and high in vivo hepatic extraction ratios.[11,19] However, it is important to remember that oral bioavailability in vivo is dependent on *both* permeability *and* first pass metabolism. If either permeability or metabolism data are considered in isolation, the result may be an inaccurate prediction of oral bioavailability.

To facilitate an effective lead candidate selection and optimization process, laboratories have sought to implement and integrate both in vitro and in vivo technologies.[20−24] Limited success is evident in the integration of in vitro Caco-2 and gut loop permeability with in vitro metabolic stability data or with the in vivo pharmacology and PK studies. Some studies did improve the PK properties for a small series of compounds in rats and guinea pigs, but they did not attempt to predict oral bioavailability in humans.

For example, Obach et al. (1997) proposed a model to predict human bioavailability, clearance, and other PK parameters from a retrospective study of in vitro metabolism and in vivo animal PK data.[25] While their model yielded acceptable predictions (within a factor of 2) for an expansive group of compounds in their database, it relied extensively on in vivo animal PK data for interspecies scaling in order to estimate human PK parameters. Because animal data are more time-consuming and costly to obtain than are permeability and metabolic clearance data, this approach may be limited to the later stages of discovery support when the numbers of compounds being evaluated are fewer.

Given the importance of integrating ADME properties early in the compound selection process, our objective was to create an intuitive, easily visualized tool to permit rapid and easy interpretation of both permeability and metabolism data. Further, this tool should not only forecast bioavailability in humans and other species but also do so at the earliest stages of the discovery process when it is still feasible for molecular redesign.

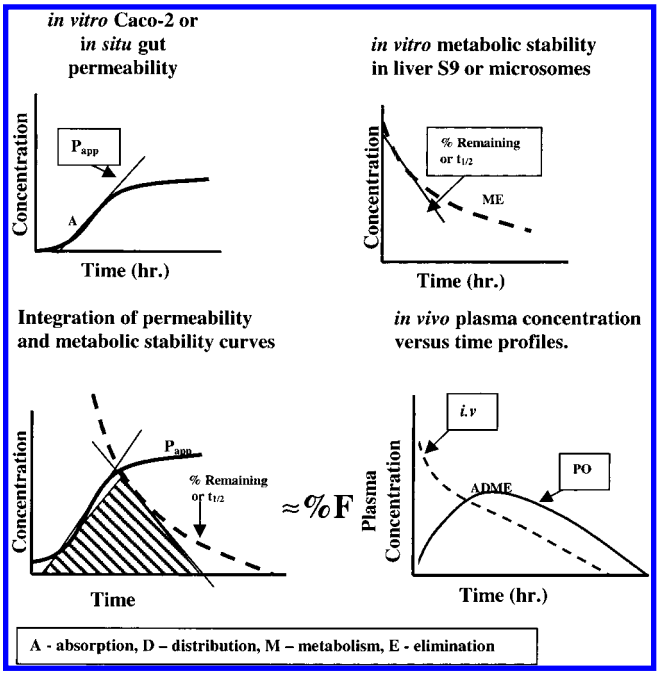

Figure 1. Integration of in vitro permeability (P_{app}) and metabolic stability data in estimating oral bioavailability (%*F*).

We propose a graphical model to categorize compounds into low, moderate, and high oral bioavailability in human and other test species by integrating the in vitro Caco-2 permeability (P_{app}) and metabolic rate of disappearance (percentage remaining, %*R*). We will demonstrate that this model applies to higher throughput in vitro permeability and metabolic stability screening systems[12] and can rapidly categorize compounds into high, medium, and low oral bioavailability in humans. Selected compounds with a high probability of success will then be evaluated by in vivo models based on potency, safety, estimated %*F* in humans, and solubility. Finally, we will demonstrate that for compounds that exhibit poor PK properties, this model provides a problem-solving tool. It will assist in organizing structure−absorption and structure−metabolism data, thereby enabling scientists to enhance absorption and metabolism properties through molecular structure manipulation, which should result in improved %*F* and half-life ($t_{1/2}$).

Model for Predicting Human Oral Bioavailability

Theoretical. The absolute oral bioavailability (%*F*) is an estimate of systemic exposure of an orally administered drug. %*F* is the key parameter along with plasma half-life ($t_{1/2}$), clearance (CL), and volume of distribution (V_d) derived from plasma concentrations of the active drug following an iv and an oral dose. %*F* is an estimate of the amount of drug that enters into the systemic circulation following oral administration, relative to an intravenous dose (eq 1). It is derived from the area under the time curve (AUC) or a plasma concentration−time profile curve by measuring the drug concentration in plasma over time (Figure 1). Thus, %*F*

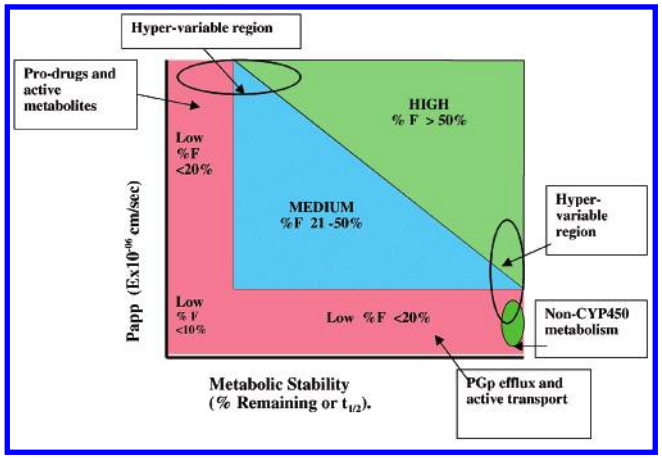

Figure 2. Graphical oral bioavailability estimation map.

is defined as the area under the curve normalized for dose.

$$\%F = \frac{\mathrm{AUC_{oral}} \times \text{iv dose}}{\mathrm{AUC_{iv}} \times \text{oral dose}} \times 100 \qquad (1)$$

The dynamic interactions between rates of absorption, metabolism, distribution, and elimination affect drug concentration in plasma following an oral dose. Drug clearance from plasma is based on the disappearance of the active drug regardless of the route of elimination, e.g., biotransformation, renal, or biliary elimination. Thus, %*F* can be viewed as an area under the curve, AUC parameter, derived from the rates of absorption and systemic clearance. When in vivo hepatic clearance is much greater than renal, biliary, and GI clearances, then the rate of hepatic clearance (metabolism) is equal to systemic clearance. Under this special circumstance, one can approximate %*F* with in vitro or in situ rates of absorption and hepatic metabolism.

On the basis of this principle, we developed a graphical model that integrates the in vitro rates of absorption and metabolic disappearance in estimating oral bioavailability (Figures 1). The rates of permeability and metabolic disappearance combine to represent a peak, whose area approximates oral bioavailability (%*F*) in humans or in any other given species. As our measure of absorption for all species, we used Caco-2 permeability (P_{app}) values because an excellent correlation between Caco-2 permeability and extent of absorption in humans and other species has already been demonstrated.[16−18] To determine the rate of metabolic disappearance, we used liver enzyme preparations from that species and determined the percentage remaining after a fixed incubation time.

Graphical Model. Species specific oral bioavailability (%*F*) estimates were derived by generating a map from an *x*, *y* plot of the in vitro rates, P_{app}, versus the rate of metabolic disappearance as expressed in the percent of drug remaining after 30 min (%*R*) or as $t_{1/2}$ (Figure 2). To generate the oral bioavailability estimation map, we employed Spotfire software, Cambridge, MA.

The plot is divided into three sections representing the low (<20%), medium (20−50%), and high (50−100%) %*F* regions (Figure 2). The low %*F* region is defined by $P_{app} < 10 \times 10^{-6}$ cm/s and 0−100% drug remaining, and by $P_{app} = 0-70 \times 10^{-6}$ cm/s and <15% parent drug remaining. We used in vitro properties of four reference compounds to define the low, medium, and high regions of the %*F* map. Verapamil and mannitol defined the boundaries for the low region, metoprolol defined the medium region, and carbamazepine defined the high region.

Validation. To test the predictive capacity of our model, this study examined 21 compounds representing 10 different therapeutic areas with a wide range of oral bioavailabilities (Table 1). Moreover, the data set available for these 21 compounds covered a variety of species, including human (eight compounds), rat (10 compounds), dog (three compounds), and guinea pig (two compounds). Of the drugs evaluated in humans, warfarin, indomethacin, and carbamazepine represented the high %*F*, timolol, verapamil, propranolol, and metoprolol represented the medium %*F*, and mannitol represented the low %*F*. In rats, dogs, and guinea pigs, five compounds were represented in high, six in medium, and five in the low %*F* region.

The criterion used to judge the utility of this model was the accuracy of assignment of drugs into their appropriate %*F* region based on their in vitro data. We defined false positive results as those compounds with predicted %*F* greater than 2× the observed value (i.e., predicted—high %*F* and observed—low %*F*). Similarly, false negatives were defined as those compounds whose predicted %*F* was a factor of 2 less than the observed value (i.e., predicted %*F* was low and observed %*F* was high).

Results

Table 1 contains the Caco-2 permeability, metabolic stability in liver S9 or microsomes, and measured %*F* values for the test compounds in human, rat, guinea pig, and dog. Further, it provides the %*F* estimates for all test compounds as derived from the bioavailability maps shown in Figures 3, 4, and 5. These figures indicate that a majority of the compounds in this test set were assigned to the correct regions of the bioavailability map. Within our data set, there were no false positives or false negatives as defined above, although two compounds along the medium and high %*F* boundary lines did show a small degree of overlap. More importantly, all low %*F* compounds were correctly placed in the low %*F* region.

Prediction in Humans. Eight compounds with available human PK data were mapped correctly into their respective %*F* regions, with no under or over predictions for this set of data (Figure 3). Warfarin (93%), indomethacin (98%), and carbamazepine (70%) were placed in the high (50−100%) %*F* region, timolol (50%), propranolol (26%), metoprolol (38%), and verapamil (22%) in the medium region (20−50%), and mannitol in the low (0−20 %*F*) region (Figure 3). Good agreement was evident between the observed and the predicted %*F* values.

Prediction in Rats, Dogs, and Guinea Pigs. All 11 compounds evaluated in animals were assigned to the correct %*F* region (Figure 3). The %*F* distribution of these compounds were as follows: three compounds with high %*F*, four compounds with medium %*F*, and four compounds with low %*F* categories (Figure 3). The

Table 1. Caco-2 Permeability, Liver S9 and Microsomal Stability, and Their Oral Bioavailabilities of Drugs in Humans, Rats, Guinea Pigs, and Dogs

compd no.	compd name	therapeutic area	metabolic stability %*R* at 30 min	Caco-2 P_{app} $\times 10^{-6}$ cm/s	oral bioavailability (%*F*)	enzyme prep.	species	observed %*F* region	predicted %*F* region	ref
1	NK1NK2 analogue 108	NK1NK2 tachykinin antagonist	30	0.1	2	S9	guinea pig	low	low	23,
2	XaI analogue 21	factor Xa inhibitor	100	2	4	S9	rat	low	low	*a*
3	NK1NK2 analogue 105	NK1NK2 tachykinin antagonist	100	5	4.9	S9	guinea pig	low	low	*a*
4	H1 analogue A	H1 antagonist	100	5	10	S9	rat	low	low	*a*
5	NK1NK2 analogue 104	NK1NK2 tachykinin antagonist	7.5	44	18	S9	rat	low	low	23
6	mannitol	diuretic	100	2	18	microsome	human	low	low	16
7	NK1NK2 analogue 212	NK1NK2 tachykinin antagonist	30	18.5	21	S9	rat	medium	medium	23
8	verapamil	Ca channel blocker	7	69.4	22	microsome	human	medium	low	15, 29
9	propranolol	β-adrenergic antagonist	29	41.9	26	microsome	human	medium	medium	15, 16, 29
10	366094	antiviral	93	10	33.2	microsome	rat	medium	medium	24
11	NK1NK2 analogue 212	NK1NK2 tachykinin antagonist	28	18.5	38	S9	dog	medium	medium	*a*
12	metoprolol	β-adrenergic antagonist	73	27	38	microsome	human	medium	medium	15, 16, 29
13	EI analogue 101	neutrophil elastase inhibitor	70	8	45.99	S9	rat	medium	low	20, 21, 22, 26, 27
14	NK1NK2 analogue 212	NK1NK2 tachykinin antagonist	47	18.5	46	S9	guinea pig	medium	medium	23
15	354400	antiviral	83	29	48.5	microsome	rat	medium	high	24
16	timolol	β-adrenergic antagonist	71	12.8	50	microsome	human	high	high	15, 31
17	NK1NK2 analogue 104	NK1NK2 tachykinin antagonist	48	44	52	S9	dog	high	mid	*a*
18	NK1NK2 analogue 104	NK1NK2 tachykinin antagonist	80	44	70	S9	guinea pig	high	high	*a*
19	carbamazepine	anticonvulsant, analgesic	96	22.8	70	microsome	human	high	high	28, 29
20	EI analogue 102	neutrophil elastase inhibitor	55	30.5	70.9	S9	rat	high	mid	20, 21, 22, 26, 27
21	341908	antiviral	89	73	79.3	microsome	rat	high	high	24
22	368177	antiviral	90	20	89.4	microsome	rat	high	high	24
23	warfarin	anticoagulant	100	38.3	93	microsome	human	high	high	30, 16
24	indomethacin	analgesic	95	20.4	98	microsome	human	high	high	15, 31

[a] See Experimental Section for details of how these data were determined.

model correctly predicts the low oral bioavailability of polar compounds (H1 analogue A, and NK1NK2 analogue 105) and positively charged quaternary amine compound (XaI analogue 21), despite their high stability to phase I metabolism. Apparently, the net estimate of oral bioavailability estimates of these compounds were still accurate because the seemingly contradictory high degree of metabolic stability was offset by their corresponding poor Caco-2 permeability. Similarly, this model correctly predicted the low %*F* of verapamil and NK1NK2 analogue 104 in rats, despite their high permeability.

Figure 4 shows the results from a larger group of NK1/NK2 analogues evaluated with this model. In vivo tests on selected compounds from each region indicate a high correlation with the actual %*F*s as determined in rats, dogs, and guinea pigs. A single compound with both low permeability and poor metabolic stability exhibits oral bioavailability of less than 2% in the rat.

Good correlation was also observed with a limited number of elastase inhibitor analogues, which had been evaluated in both in situ gut loop and Caco-2 permeability absorption models. Our study obtained identical %*F* estimates when permeability values from either in situ gut loop or Caco-2 permeability were used (Figure 5).

Discussion

Traditionally, lead compounds are deselected in development based on toxicity or lack of efficacy. If used at all, ADME data is used retrospectively as a tool for "post mortem" analysis to understand compound failures rather than being used prospectively to forecast in vivo effects. For example, ADME data can explain poor oral absorption, high first pass metabolism, or rapid systemic clearance resulting in low bioavailability. Similarly, an explanation for toxicity effects through the analysis of the CYP450 biotransformation or enzyme

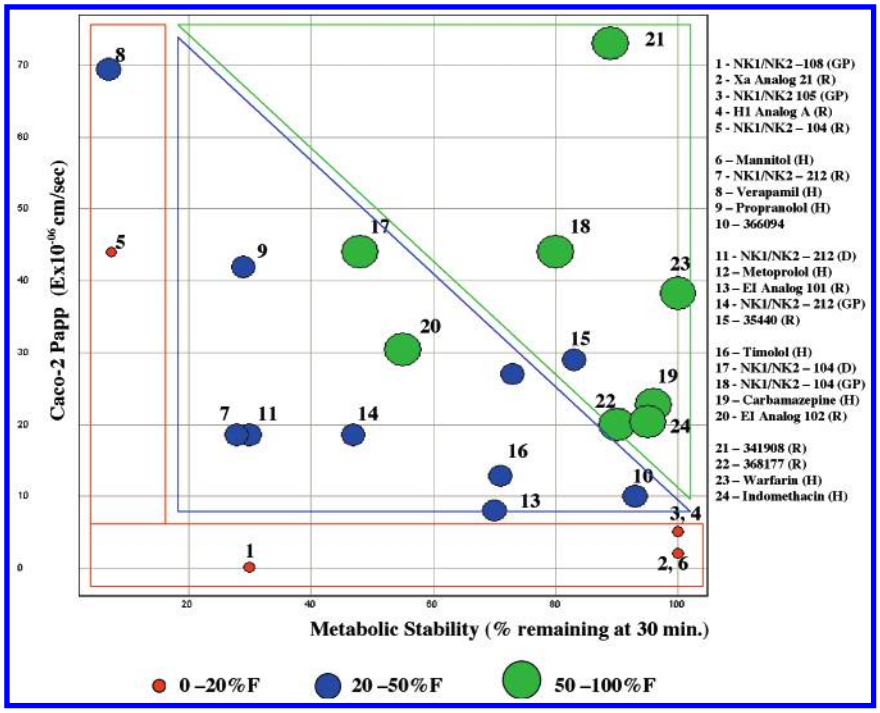

Figure 3. Oral bioavailability estimates of drugs in rats, guinea pig, dog, and human from their respective Caco-2 P_{app} and metabolic stability in liver microsomes or S9. Data points are sized by oral bioavailability (%*F*) in humans, rats, guinea pigs, and dogs.

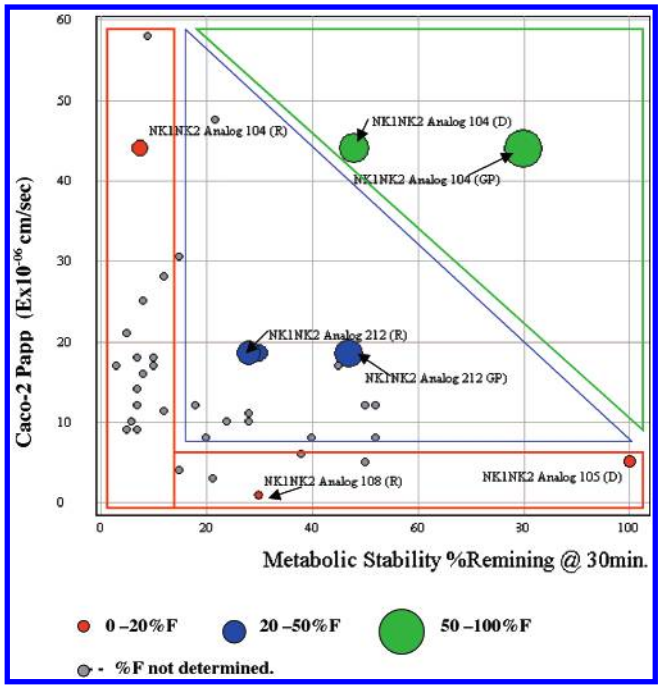

Figure 4. Oral bioavailability estimates of NK1NK2 analogues from their Caco-2 P_{app} and metabolic stability in liver S9 of rats, dogs, and guinea pigs. Data points are sized by oral bioavailability (%*F*) in rats, guinea pigs, and dogs.

inhibition can prospectively predict the outcome. Thus, there is a need for timely in vitro estimates of systemic exposure (oral bioavailability), first pass metabolism, and CYP450 inhibition for potential lead compounds in the early discovery stage to enhance the selection of compounds for in vivo evaluations.

This does not suggest that such data should be used exclusively as a criterion to select or deselect compounds. Rather, compound selection for in vivo evaluations should be based on potency, lack of toxicity, physical properties, and estimated systemic exposure (oral bioavailability and clearance). Moreover, a systematic process would provide timely information to assist medicinal chemists in structure modification. This in turn allows early optimization of solubility, permeability, and metabolism properties for compounds that exhibit poor PK properties.

The graphical model described, upon retrospective analysis of a defined set of in vitro and in vivo PK data, appears to be able to correctly assign bioavailability values. This model is not used to predict the precise PK parameters but rather to rapidly forecast whether the compound will have satisfactory or unsatisfactory oral bioavailability in humans and in animals. The graphical model enables a scientist to obtain species-specific oral bioavailability estimates for a large variety of compounds with the nonlinear approach. The consequence of a linear approach (rank order) based on a single parameter, such as fraction dose absorbed or the rate of metabolism (microsomal or hepatic intrinsic clearance), is that it will not reconcile the %*F* for highly absorbed and highly metabolized drugs or for poorly absorbed and slowly metabolized drugs.

A benefit of this model is that it may assist in the organization of structure−absorption/metabolism/physical property data to enhance solubility, absorption, and metabolism properties. Thus, it may result in improved systemic exposure (%*F*) and half-life. Also, this approach provides a rational and efficient means of utilizing the limited in vivo resources for evaluating potential lead compounds that have a higher probability of success in development. Our intent is to use this predictive model in conjunction with a high throughput in vitro ADME screening system to aid in a rational lead selection and optimization process.[12]

Challenges in Optimizing ADME Properties of Leads. Permeability and metabolism often have oppos-

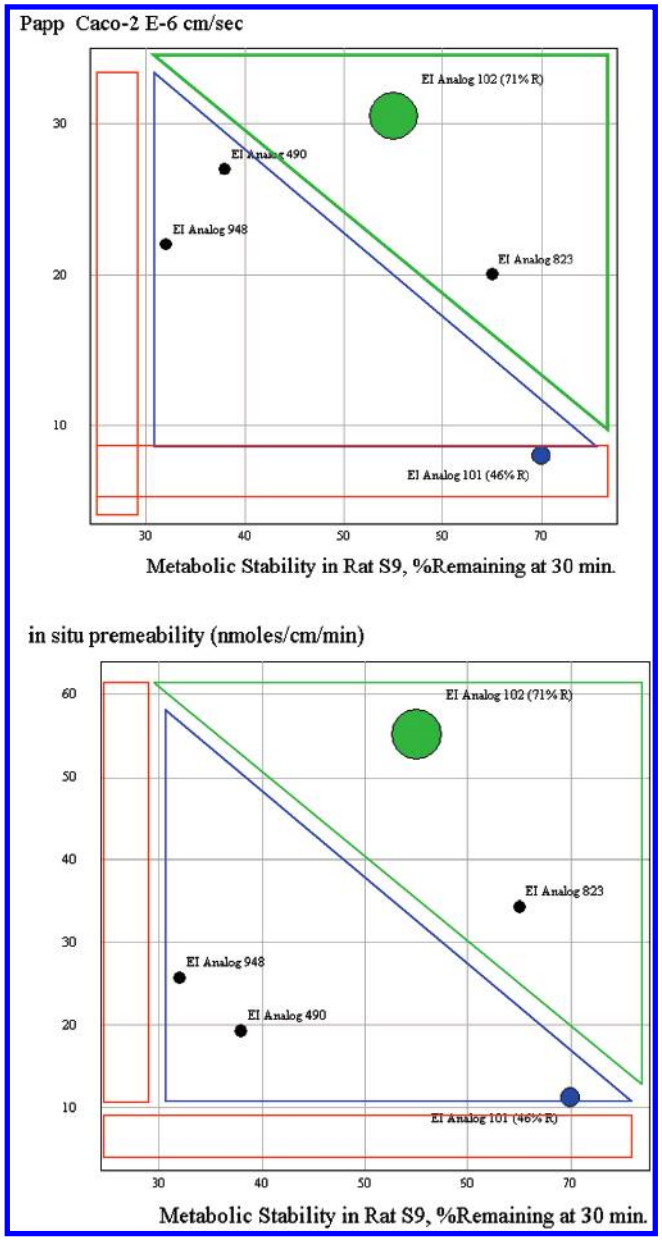

Figure 5. Oral bioavailability of elastase inhibitors in rats and the estimated relative bioavailability based on Caco-2 and in situ gut permeability−liver S9 metabolic stability in rats. Black data points: %*F* not determined.

ing structural requirements. Optimizing permeability and metabolic stability properties concurrently with solubility and potency (binding affinity IC_{50} and K_i) through structure modification is very complex. In general, lipophilic compounds tend to be more permeable. They also tend to make good substrates for CYP450 enzymes, resulting in rapid metabolism and consequently low %*F*.[10] In contrast, polar or ionizable (anionic and cationic) compounds tend to be metabolized by phase II conjugative or cytosolic enzymes or excreted unchanged in vivo. Consequently, these compounds typically exhibit high stability in microsomal or S9 incubations. These compounds will also exhibit low permeability in the Caco-2 model due to their polarity or ionization at neutral pH.

Further, solving metabolic stability problems at one site may result in the increase in the rate of metabolism at another site, a phenomenon known as "metabolic switching." Thus, structure modifications to solve a metabolic stability problem may not necessarily lead to a compound with an overall improvement in PK properties. In addition, the reduction in metabolic (hepatic) clearance may lead to increased renal or biliary clearance of the parent drug or inhibition of one or more drug-metabolizing enzymes.

An apparent improvement of an in vitro metabolism property may not result in improved in vivo performance, since the compound may exhibit saturable metabolism, nonlinear PK, or drug−drug interactions. It is recommended that in vitro metabolic stability data be integrated with inhibition screening. Essentially, one must include in vitro human ADME data to optimize lead candidates in animals. The design of drugs with optimal potency and PK properties is extremely challenging given the opposing requirements for absorption and metabolism as well as the general lack of sufficient in vitro and in vivo data sets for a large diversity of compounds.

The first step in the lead optimization process is to thoroughly explore the structural requirements for in vitro pharmacological activity. By combinatorial synthesis, one may identify the key structural features that are essential for activity. The next step is to attempt to improve the permeability and metabolism properties through structure modifications to the regions of the molecule that have little or no impact on the activity. A scientist may maintain a desired level of potency while introducing structural features that will improve the metabolism and permeability characteristics. To serve as a preclinical "proof-of-concept," it may be prudent to evaluate a small number of compounds with good potency and moderate oral bioavailability through in vivo pharmacological models at early stages in the optimization process. The "proof-of-concept" test need only produce a desired physiological or biochemical effect that is consistent with pharmacological activity. This prevents a great deal of optimization effort on a series of compounds that have no in vivo activity.

Model Limitations and Applications. Note some precautions in the use of this graphical approach. First, a premise in this model is that permeability and metabolic clearance is more important than renal or biliary clearance to determine the %*F* for these diverse groups of compounds. Despite the lack of in vitro renal or biliary clearance or protein binding data, one still obtains good estimates of %*F* with this model. Next, physicochemical data, such as solubility, log *P*, and pK_a still have a significant involvement in conjunction with a predictive PK model and in the selection of compounds for subsequent in vivo pharmacology or PK studies. Further, the model's predictability is best applied to passively diffused compounds, which accounts for approximately 80% of all compounds. The model may underestimate the %*F* for actively transported compounds, and there is a limited means to directly account for efflux or active transport from simple unidirectional permeability data.

Model variability occurs when compounds fall into the two hyper-variable regions in the %*F* map or where all three %*F* regions converge (Figure 2). In these cases, bioavailability could easily be under- or overestimated if there is even a small degree of variance in the P_{app} or

%*R* determinations. For example, compounds which are found in the lower right hyper-variable region and might exhibit this kind of variability include small polar compounds, larger compounds with carboxylic acid, or charged functional groups. Similarly, when ester pro-drugs and highly lipophilic compounds are present in the upper left hyper-variable region, there may also be a higher degree of variability.

NK1/NK2 analogues such as 105 (#3), which has a carboxylic acid group, and 104 (#5), an ester derivative, illustrate the strong interlink between permeability and metabolism on oral bioavailability. Analogue 105 had complete stability in S9, as it is not metabolized by CYP450, but also had low permeability due to its net negative charge at pH 6.5−7.0 in Caco-2 studies. With the elimination of ionization through esterification, the permeability of the analogue 105 is increased approximately 8-fold.

While the ester pro-drug (NK1/NK2 analogue 104) indicated high permeability, it also undergoes rapid hydrolysis. Consequently, the analogue had lower %*F* in rats. However, the ester moiety of this compound is hydrolyzed to a much lesser extent in dogs and guinea pigs, resulting in higher oral bioavailability in these two species. Thus, it is prudent to evaluate compounds that have high permeability and low metabolic stability or vice versa in detail during both in vitro/in situ and in vivo evaluations.

Secondary in vitro ADME screens may potentially assist in the determination of several variables. Key variables such as stability in hepatocytes, blood, and plasma; metabolite and metabolic pathway identification; active transport; and Pgp efflux in cell cultures—across gut segments or in gut loop models—are important dimensions for bioavailability. Further, in vivo pharmacology screens for activity may be necessary since some compounds may exert activity through potential active metabolites.

By testing a larger set of structural analogues from the NK1/NK2 project with this model, we observed a narrow distribution within an estimated %*F* region. This is probably due to the similarities in their physicochemical properties, which play an important role in both permeability and metabolism (Figure 4). However, structural analogues with a wide range in physicochemical properties and varying functional substitutions do show a large variance in both permeability and metabolic clearance and hence in their %*F* (Figure 5). It is interesting to note that similar %*F* estimations were obtained with gut loop and Caco-2 permeability models for a small number of elastase inhibitor analogues (Figure 5).

Conclusion

We have demonstrated and described an intuitive, graphical model for estimating oral bioavailability in humans and three other species from in vitro data, without the need of in vivo interspecies scaling. We demonstrated the predictive capacity and the utility of this model with 21 structurally diverse compounds from 10 different therapeutic areas with a wide range of %*F* values in humans, rats, dogs, and guinea pigs. The main utility of this graphical model in combination with a high throughput in vitro ADME screening system is to rapidly classify compounds into groups of low, medium, and high %*F* in humans or any other species. This model provides a rational and efficient alternative means of utilizing resources for evaluating the oral bioavailability of potential lead compounds. Further, this process provides timely information to the medicinal chemist for structure modification to optimize solubility, permeability, and metabolism properties for compounds that exhibit poor PK properties. In addition, it enables one to focus on promising compounds that have a higher probability of success in development, thus accelerating the lead compound selection process. In conclusion, this graphical model is a rapid and facile tool for the rational selection of compounds with optimal ADME properties in humans. Thus, use of this model could potentially help accelerate drug discovery programs by advancing compounds with a higher degree of success in humans.

Experimental Section

Sources of Pharmacokinetic and in Vitro Data. Oral bioavailability data for humans was obtained from Goodman and Gilman's "The Pharmacological Basis of Therapeutics,"[28] whereas similar animal data were obtained from the literature.[21−24] In vitro permeability and metabolism data were either generated within our laboratory or reported in the literature[15,16,20−24,26−31] (Table 1).

In Vitro Permeability Experiments. All permeability studies conducted were performed with Caco-2 monolayers as described previously.[20,23,24,26,29,31] Caco-2 cells were cultured in supplemented Dulbecco's modified eagle medium with 10% fetal bovine serum and seeded onto polycarbonate membranes for test compound transport experiments. Caco-2 cell membranes were grown by seeding on Snapwell supports maintained in an incubator at 37 °C with 5% CO_2/95% O_2 and approximately 95% humidity for 21 to 30 days. Drug permeability experiments were conducted at 37 °C by adding 10−30 μM drug solution in HEPES buffer (pH 7.4) to the apical (donor side) of the monolayer. All compounds were solubilized in HEPES buffer and remained in solution during Caco-2 permeability measurements. Compounds with a solubility of less than 10 μM in HEPES buffer were not tested. Samples were obtained from the apical (donor) side at zero (0) time point and from the basolateral (receiver side) chamber at time points of 0, 15, 30, 45, 60, 90, 120, 180, and 240 min after addition of test compound. Samples were snap frozen on dry ice/methanol. Drug concentrations were determined by liquid chromatography with ultraviolet (LC/UV) or mass spectral (LC/MS) analysis. Phenytoin and mannitol were evaluated as positive and negative controls. Caco-2 apparent permeability values (P_{app}) were calculated as follows

$$P_{app}(\text{cm/s}) = (dQ/dt)(1/A)(1/C_0)$$

where dQ/dt was the rate of appearance of the drug in the receiver chamber, C_0 was the initial concentration of the drug in the donor chamber, and A was the surface area of the monolayer. All P_{app} values were standardized and reported as $\times 10^{-06}$ cm/s. (Table 1).

In Vitro Metabolism Experiments. Metabolic stability studies were conducted with isolated liver S9 or microsomes from human (pooled), rat, dog, and guinea pig, as described previously.[15,22−24,30] Metabolic stability values for several compounds in Table 1 have not been previously reported. Data for these compounds was generated as follows. All substrates were incubated at 37 °C, pH 7.4. The reaction mixture consisted of 4 mL of a 5 mg protein/mL suspension of liver S9 (equivalent to approximately 1 mg/mL of microsomal protein in the final reaction mixture), 4 mL of an NADPH generating cofactor (6.4 mM glucose-6-phosphate, 1.1 mM NADP, and 1.3 mM $MgSO_4$), 0.32 mL of glucose-6-phosphate dehydrogenase, 7.58 mL of 0.1 N K_2HPO_4, and 0.1 mL of substrate

(6−8 μg/mL) such that the concentration was 10 μM in the final reaction volume of 16 mL. Triplicate aliquots (0.5 mL) were removed from each incubation beaker at time points of 1, 3, 5, 10, 15, 30, and 60 min. All samples were snap frozen in a hexane/dry ice slurry to instantaneously deactivate the enzymes. Samples were stored at −70 °C until assayed.

Drug concentrations were determined by LC/UV or LC/MS analysis. The rate of drug disappearance was expressed as percent of parent drug remaining at 30 min (%*R*) or as half-life ($t_{1/2}$). %*R* was calculated as follows:

$$\%R = (C_{30}/C_0) \times 100$$

where C_0 and C_{30} were the drug concentrations in the S9 or microsomal incubation mixture at time points of 0 and 30 min, respectively. Although either %*R* or half-life ($t_{1/2}$) could be used in estimating %*F*, we choose %*R* to standardize our laboratory values with those reported in the literature (Table 1).

In Vivo Studies. Absolute oral bioavailability was determined following oral and intravenous (iv) administration of compounds to rats, guinea pigs, or dogs. Compounds were administered either as a solution or a suspension. Plasma concentrations of the parent compounds were quantitated by LC−UV or LC/MS analysis. Absolute oral bioavailability was calculated from plasma $AUC_{0-\infty}$ of the parent drug as shown in eq 1.

Oral Bioavailability Estimation Plot. Species-specific oral bioavailability estimations were derived by plotting %*R*, the rate of metabolic disappearance, along the *x* axis and the Caco-2 P_{app} values along the *y* axis (Figure 2) using Spotfire software, Cambridge, MA. The data points on the *x*,*y* plots were sized by their respective experimental %*F* values and color coded either red for low, blue for medium, or green for high %*F* bin assignment. Verapamil, mannitol (low), metoprolol (medium), and carbamazepine (high) were used as reference compounds to define the boundaries of the %*F* regions.

References

(1) Sietsema, W. K. The absolute oral bioavailability of selected drugs. *Int. J. Clin. Pharmacol., Ther. .Toxicol.* **1989**, *27* (4), 179−211.

(2) Prentis, R. A.; Lis, Y.; Walker, S. R. Pharmaceutical innovation by the seven UK-owned pharmaceutical companies (1964−1985). *Br. J. Clin. Pharmacol.* **1988**, *25*, 387−396.

(3) Kennedy, T. Managing the drug discovery/development interface. *Drug Discovery Today* **1997**, *2* (10), 436−444.

(4) Berman, J.; Halm, K.; Adkison, K.; Shaffer, J. Simultaneous pharmacokinetic screening of a mixture of compounds in the dog using API LC/MS/MS analysis for increased throughput. *J. Med Chem.* **1997**, *40*, 827−829.

(5) Olah, T. V.; McLoughlin, D. A.; Gilbert, J. D. The simultaneous determination of mixtures of drug candidates by liquid chromatography/atmospheric pressure chemical ionization mass spectrometry as an in vivo drug screening procedure. *Rapid Commun. Mass Spectrom.* **1997**, *11*, 17−23.

(6) Bryant, M. S.; Korfmacher, W. A.; Wang, S. Y.; Nardo, C.; Nomeir, A. A.; Lin, C. C. Pharmacokinetics screening for the selection of new drug discovery candidates is greatly enhanced through the use of liquid chromatography atmospheric pressure ionization tandem mass spectrometry. *J. Chromatogr.* **1997**, *777*, 61−66.

(7) Lipinski, C. A.; Lombardo, F.; Dominy, B. W.; Feeney, P. J. Experimental and computational approaches to estimate solubility and permeability in drug discovery and development settings. *Adv. Drug Delivery Rev.* **1997**, *23*, 3−25.

(8) Artursson, P.; Katrin, P.; Luthman, K. Caco-2 monolayers in experimental and theoretical predictions of drug transport. *Adv. Drug Delivery Rev.* **1996**, *22*, 67−84.

(9) Delie, F.; Rubas, W. A human colonic cell line sharing similarities with enterocytes as a model to examine oral absorption: Advantages and limitations of the Caco-2 model. *Crit. Rev. Ther. Drug Carrier Syst.* **1997**, *14* (3), 221−286.

(10) Smith, D. A. Design of drugs through a consideration of drug metabolism and pharmacokinetics. *Eur. J. Drug Metab. Pharmacokinet.* **1994**, *3*, 193−199.

(11) Iwatsubo, T.; Hirota, N.; Ooie, T.; Suzuki, H.; Shimada, N.; Chiba, K.; Ishizaki, T.; Green, C.; Tyson, C.; Sugiyama, Y. Prediction of *in vivo* drug metabolism in the human liver from in vitro metabolism data. *Pharmacol. Ther.* **1997**, *73* (2), 147−171.

(12) Mandagere, A. K.; Kibbey, C.; Narayanan, S.; Michael, S.; Sinz, M.; Stilgenbauer, L.; Quimby, A.; Woodhams, P.; Wu, S.; Qin, R.; Mei, H. Y.; Thompson, T. N.; Hwang, K. K. *Automated Higher Throughput in vitro ADME Screening System in Drug Discovery and Development*; Millennial World Congress of the Pharmaceutical Sciences: San Francisco, CA, 2000.

(13) Mandagere, A. K.; Correll, M. A.; Mooney, J. P.; Poole, J. C.; Hwang, K. K.; Cheng, L. K. Application of automation to Caco-2 drug diffusion studies. *Pharm. Res.* **1996**, *13*, S237.

(14) Garber, P.; Eriksson, P.; Schipper, N.; Sjostrom, B. Automated absorption assessment using Caco-2 cells cultured on both sides of polycarbonate membranes. *Pharm. Res.* **1999**, *16* (3).

(15) Ho, J. C.; Brown, P. W.; Emary, W. B.; Thompson. T. N.; Toren, P. C.; Yerino, P. P. *Higher throughput metabolic stability screen*; Annual AAPS conference: New Orleans, 1999.

(16) Arthursson, P.; Karlsson, J. Correlation between oral drug absorption in humans and apparent drug permeability coefficients in human intestinal epithelial (Caco-2) cells. *Biochem. Biophys. Res. Commun.* **1991**, *175* (3), 880−885.

(17) Rubas, W.; Villagran, J.; Cromwell, M.; McLeod, A.; Wassenberg, J.; Mrsny, R. Correlation of solute flux across Caco-2 monolayers and colonic tissue in vitro. S. T. P. *Pharm. Sci.* **1995**, *5* (1), 93−97.

(18) Chiou, W. L.; Barve, A. Linear correlation of the fraction of oral dose absorbed of 64 drugs between humans and rats. *Pharm. Res.* **1998**, *15* (11), 1792−1795.

(19) Lave, T.; Dupin, S.; Schmitt, Valles, B.; Ubeaud, G.; Chou, R. C.; Jaeck, D.; Coassolo, P. The use of human hepatocytes to select compounds based on their expected hepatic extraction ratios in humans. *Pharm. Res.* **1997**, *14* (2).

(20) Hwang, K. K.; Thompson, T. N.; Cheng, L. Strategy for selection of a drug candidate with optimal bioavailability from a series of analogs. *Pharm. Res.* **1996**, *13* (9), S-237.

(21) Janusz, M. J.; Durham, S. L.; Hare, C. M.; Geary, J. L.; Mandagere, A. K.; Poole, J. C.; Thompson, T. N.; Xu, D.; Angelastro, M. R.; Burkhart, J. P.; Chen, T. M.; Marquart, A. L.; Peet, N. P.; Hwang, K. K. Pharmacological evaluation of selected, orally active peptidyl inhibitors of human neutrophil elastase. *J. Pharmacol. Exp. Ther.* **1995**, *275*, 1233−1238.

(22) Thompson, T. N.; Correll, M. A.; Geary, J. L.; Mandagere, A. K.; Mooney, J. P.; Poole, J. C.; Xu, D.; Yerino, P. P.; Hwang, K. K. *Selection of an elastase inhibitor with improved bioavailability from a series of structurally related analogues*; ISSX: 1996.

(23) Burholder, T. P.; Kudlacz, E. M.; Maynard, G. D.; Liu, X. G.; Le, T. B.; Bratton, L.; Webster, M. E.; Horgan, S. W.; Wenstrup, D. L.; Freund, D. W.; Boyer, F.; Gross, R. S.; Knippenberg, W.; Logan, D. E.; Jones, B. K.; Chen, T. M.; Geary, J. L.; Correll, M. A.; Poole, J. C.; Mandagere, A. K.; Thompson, T. N.; Hwang, K. K. Chemical synthesis and structure activity relationships for a series of substituted pyrrolidine NK1/NK2 receptor antagonists. *Bioorg. Med. Chem. Lett.* **1997**, *7* (19), 2531−2536.

(24) Stratford, R. E.; Clay, M. P.; Heinz, B. A.; Kuhfeld, M. T.; Osborne, S. J.; Phillips, D. L.; Swetana, S. A.; Tebbe, M. J.; Vasudevan, V.; Zornes, L. L.; Lindstrom, T. D. Application of oral bioavailability surrogates in the design of orally active inhibitors of Rhinovirus replication. *J. Pharm. Sci.* **1999**, *88* (8), 747−753.

(25) Obach, R. S.; Baxter, J. G.; Liston, T. E.; Silber, M, R.; Jones, B. C.; MacIntyre, F.; Rance, D. J.; Wastall, P. The prediction of human pharmacokinetic parameters from preclinical and in vitro metabolism data. *J. Pharmacol. Exp. Ther.* **1997**, 283, 46−58.

(26) Hwang, K. K.; Poole, C.; Correll, M. Caco-2 cells as an in vitro model for the prediction of GI absorption from a series of peptidyl inhibitors of human neutrophil elastase. *Pharmaceut. Res.* **1996**, *13* (9), S-236.

(27) Hwang, K.-K.; Yerino, P. Using rat jejunal muscosa diffusion cell model to select an elastase inhibitor with optimal GI permeability from a series of structurally related analogs. *Pharm. Res.* **1995**, *12* (9), S-290.

(28) *The Pharmacological Basis of Therapeutics*, 8th ed.; Gilman, A. G., Rall, T. W., Nies, A. S., Taylor, P., Eds.; Pergamon Press: New York, 1990; pp 1655−1715.

(29) Withington, L.; Asa, D. *Comparison of compound permeability measurements using various culturing modifications of the Caco-2 line*; Annual AAPS conference: New Orleans, 1999.

(30) Zhang, K. E.; Pelimiano, M.; Hee, B. R.; Shetty, B. *Validation of a streamlined in vitro metabolic stability screening assay*; Annual AAPS conference: New Orleans, 1999.

(31) Yazdanian, M.; Glynn, S. L.; Wright, J. L.; Hawi, A. Correlation partitioning and Caco-2 cell permeability of structurally diverse small molecular weight Compounds. *Pharm. Res.* **1998**, *15* (9).

JM010152K